Pergamon

Acta Astronautica Vol. 34, pp. 17–23, 1994
Elsevier Science Ltd. Printed in Great Britain

0094-5765(94)00046-8

FISSION OR FUSION FOR MARS MISSIONS: EXPECTATIONS AND CHALLENGES

Terry Kammash*

University of Michigan
Ann Arbor, MI, U.S.A.

Abstract

A fission based system in the form of the Gas Core Nuclear Rocket (GCR) and a laser-driven inertial fusion system that utilizes a self-generated magnetic field (MICF) are compared as potential propulsion systems for manned planetary travel. The first generates thrust by a hydrogen propellant that is heated by radiation emitted from a critical reactor with a uranium fuel in plasma form, to take advantage of high achievable temperatures. The fusion system produces attractive propulsion characteristics through energy magnification of a hot hydrogenous plasma which is guided by a magnetic nozzle that allows thermal energy to be converted into thrust. Although both systems are capable of producing several thousand seconds of specific impulse, and tens to hundreds of kilonewtons of thrust, each faces some formidable physics and engineering problems that must be addressed if they are to become viable propulsion systems. With the aid of an appropriate set of fluid and plasma equations, we assess the dynamics of each system and identify those issues that could detract from their performance. In the case of GCR, thermal hydraulic considerations reveal deterioration of propulsive capability when wall heat flux limitations and turbulent mixing are taken into account. Moreover, hydrodynamics and acoustic instabilities could also adversely affect its performance, although they may be amenable to stabilization by magnetic fields. For MICF, large energy multiplication at modest input laser energies appears to be a major concern, but if anti-hydrogen can be used to initiate the fusion reactions, this concept can be truly an outstanding propulsion device.

Nomenclature

A_0	Nozzle throat area
B	Magnetic field strength
C	Constant in Eq. (22)
C_{ph}	Specific heat
C_{sr}	Sound speed at the reservoir in MICF
D	Distance between end points of interplanetary trip
e	Subscript denoting electrons in MICF
E	Mean energy
f	Subscript denoting fuel ions in MICF
F	Rocket thrust
g	Earth's gravitational acceleration
g	Acceleration associated with external forces
h	Subscript denoting hydrogen propellant in GCR
I_{sp}	Specific impulse of rocket engine
k	Heat transfer coefficient
k_c	Critical wave number
k_R	Mean Rosseland absorption coefficient
k_v	Oscillation wave number
M	Mass of a uranium atom
n	Density of neutrons in GCR
n_f	Number density of fuel ions in MICF
N_U	Number density of uranium fuel ions in GCR
p_f	Fluid pressure
P_f	Fission power density in GCR
q	Heat flux
Q	Energy enhancement factor in MICF
r	Radial position
R_M	Mirror Ratio for magnetic mirror confinement
$\vec{\vec{S}}$	Stress tensor
t	Time
T	Temperature
U	Subscript denoting uranium in GCR
$\vec{v}$	Velocity vector
v_s	Sound speed in the uranium plasma in GCR
V	Average neutron velocity in GCR
W	Energy transport across magnetic field in MICF
W_f	Dry weight of space rocket
$\vec{x}$	Position vector
z	Axial position
Z_U	Effective charge number of the uranium ions
α	Constant in Eq. (5)
γ	Adiabatic constant
Γ	Particle flux across magnetic field in MICF
K	Boltzmann Constant
K_R	Radiation diffusion coefficient
λ_c	Critical wavelength
ϕ	Neutron flux in GCR
Φ	Electrostatic potential in GCR core
ρ	Mass density
σ	Neutron-induced fission cross section
σ_B	Black body constant
τ_{RT}	Round trip travel time of interplanetary trip
τ_U	Uranium ion confinement time in GCR
ω	Oscillation frequency in GCR Repetition rate of MICF engine
ω_i	Instability growth rate
$(n\tau)$	Energy exchange parameter in MICF
$<\sigma v>$	Velocity-averaged fusion cross section

Introduction

Man's attempt to explore space requires propulsion devices with performance capabilities that far exceed those provided by chemical propulsion, electric propulsion, or even solid core nuclear thermal propulsion, since the maximum specific impulse, I_{sp}, these systems can deliver is less than a thousand seconds. High propulsive characteristics are needed since space travel is hazardous, and man is unable to endure long journeys without experiencing physical and mental degradation. It is suggested, for example, that in order for a moderately sized vehicle to make a round trip to Mars in a few months instead

* Professor of Nuclear Engineering and Senior Member AIAA

of a few years, a propulsion system must generate several thousand seconds of specific impulse and tens to hundreds of kilonewtons of thrust, F. For the sake of dramatizing the capabilities of the two systems we will examine in this paper, we adopt a continuous burn (constant thrust) acceleration/deceleration trajectory profile which yields for the round trip travel time, τ_{RT}, between two points separated by a linear distance D the result(1)

$$\tau_{RT} = \frac{4D}{g I_{sp}} + 4\sqrt{\frac{D W_f}{gF}} \qquad (1)$$

where g is the earth's gravitational acceleration and W_f is the dry weight of the vehicle. It is clear from the above expression that the travel time can be shortened by increasing both I_{sp} and F, with greater sensitivity to the specific impulse. It is equally clear that these stringent requirements can only be met by a nuclear-based advanced propulsion system. Two likely candidates are the open cycle Gas Core Fission Rocket (GCR), and a novel inertial confinement fusion concept known as the Magnetically Insulated Inertial Confinement Fusion (MICF) reactor.

The principle of operation in GCR(2) involves a critical uranium core in the form of a gaseous plasma that heats, through radiation, a seeded hydrogen propellant which then exits through a nozzle, thereby converting thermal energy into thrust as demonstrated in Fig. 1. The MICF(3) is a fusion scheme that combines the favorable aspects of inertial and magnetic fusions into one where physical containment of the hot plasma is provided by a metal shell, while its thermal energy is insulated from this wall by a strong, self-generated magnetic field as illustrated in Fig. 2. The fusion nuclear reactions in this device are triggered by a laser beam that enters the target through a hole and ablates the deuterium-tritium (DT) - coated inner wall to form the plasmas core at the center. The burn time is dictated by the time it takes the shock wave initiated at the inner wall to reach the outer surface, and that is typically 10^{-7} seconds(4). For properly designed targets, an energy magnification of several hundred can be achieved, which in turn can result in very attractive propulsion parameters as will be noted shortly.

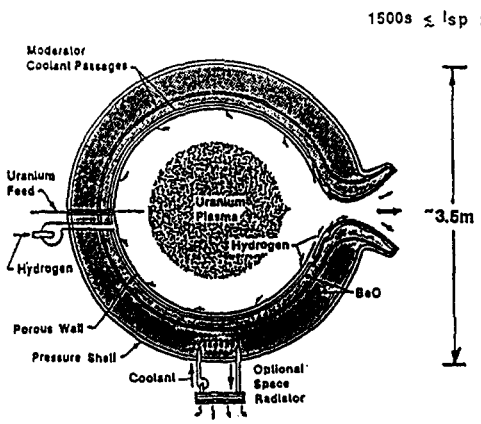

Fig. 1. High Specific Impulse, Porous Wall Gas Core Engine. (Courtesy of NASA, Lewis Research Center)

In order to circumvent the temperature limitations imposed by material melting encountered in solid core nuclear thermal propulsion, the fuel in GCR is allowed to exist in a high temperature ($10^{4°}$ K - $10^{5°}$ K) partially ionized state, and must be formed at a relatively high pressure (500 - 1000 atm) to achieve criticality in a moderately small volume. With this concept, specific impulse values ranging from 1500 to 7000 seconds appear to be feasible(2). As shown in Fig. 1, the open cycle GCR is basically spherical in shape and contains three solid regions: an outer pressure vessel, a neutron moderator/reflector, and an inner porous liner. The hydrogen propellant is injected through the porous wall with a flow distribution that creates a relatively stagnant non-recirculating central fuel region in the cavity. It has been suggested that a small amount of fissionable fuel (up to 1% of the hydrogen mass flow rate) gets exhausted along with the heated propellant under normal conditions. It is also noted that due to the transparency of both the uranium plasma and the hot hydrogen, 7 - 10% of the total reactor power appears as a radiation which is ultimately deposited principally in the solid regions of the reactor wall. It is the ability to remove this energy, either by means of an external radiator or regeneratively using the hydrogen propellant, that determines the maximum power output and achievable specific impulse for GCR engines. This will be borne out by the analysis that follows.

Analytical Modeling of GCR

We begin by examining the dynamics of the fuel core in GCR. Assuming a singly ionized uranium plasma that

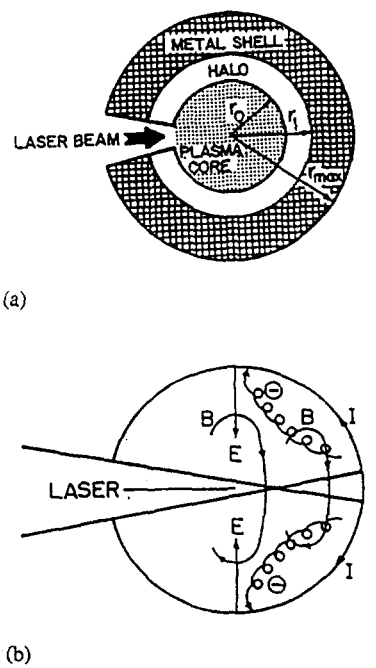

Fig. 2
Schematic Diagram of (a) Plasma Formation and (b) Magnetic Field Formation in MICF

remains so at all times, the appropriate conservation equations for the system may be written as[6]

$$\frac{\partial N_U}{\partial t} + \frac{\partial}{\partial \vec{x}}\cdot(N_U\vec{v}) = 0 \qquad (2)$$

$$\frac{\partial \vec{v}}{\partial t} + \vec{v}\cdot\frac{\partial \vec{v}}{\partial \vec{x}} + MN_U\frac{\partial}{\partial \vec{x}}[2N_U kT] = 0 \qquad (3)$$

$$\left(\frac{\partial}{\partial t} + \vec{v}\cdot\frac{\partial}{\partial \vec{x}}\right)(3N_U kT) + [5N_U kT]\frac{\partial}{\partial \vec{x}}\cdot\vec{v} = P_f + \frac{\partial}{\partial \vec{x}}\cdot\left(K_R\frac{\partial T}{\partial \vec{x}}\right) \qquad (4)$$

where N_U is the number density of the uranium ions, $\vec{v}$ the fluid velocity, T the temperature, and M is the mass of the uranium ion. The above equations become a closed system when we specify the fission power density, namely

$$P_f = N_U n V \sigma Q = \alpha\phi\rho_U \qquad (5)$$

and the radiation diffusion coefficient

$$K_R = \frac{16\sigma_B T^3}{3k_R} \qquad (6)$$

In the above equations, n is the number density of the neutrons, V their average velocity, ϕ their flux, σ the cross section for neutron-induced fission, and Q the energy released as fragment kinetic energy per fission. In the second form of P_f, the quantity α is in effect a constant, while $\rho_U = MN_U$ is the mass density of the uranium. Eq. (6) gives an effective diffusion coefficient for the radiative energy term shown at the end of Eq. (4). The quantity σ_B is the black body constant and k_R the mean Rosseland absorption coefficient.

The first problem we address with the above equations is the acoustic instability which arises from density fluctuations that result in an increase in the power density in some region of the core. Competing with this process is the fact that radiation tends to transport the extra thermal energy out of that region. By linearizing the conservation equations about the equilibrium parameters N_{U0}, T_{U0}, and $\vec{v}_0 = 0$, and assuming that the perturbed quantities vary in space and time as

$$N_1, v_1, T_1 \sim \exp(i[\vec{k}_V\cdot\vec{x} - \omega t]) \qquad (7)$$

where k_V and ω are respectively the wave number and frequency of the oscillation, we derive a dispersion equation relating k_V to ω and obtain for the growth rate, ω_I, the result is

$$\omega_I = \frac{\{2P_f/M - k_V^2 K_R[v_s^2 - 2KT_{U0}/M]/K\}}{6N_{U0}v_s^2} \qquad (8)$$

where v_s is the sound speed in the uranium plasma, given by

$$v_s = \left(\frac{10KT_{U0}}{3M}\right)^{1/2} \qquad (9)$$

and K is the familiar Boltzmann Constant. We note from Eq. (8) that a positive numerator gives rise to an instability, and the critical wave number k_C is express by

$$k_C = \left[\frac{3P_f}{2T_{U0}K_R}\right] = \frac{2\pi}{\lambda_C} \qquad (10)$$

If we apply these results to a commonly noted GCR design[7], whose core radius is 1 m, in a 7.5 GW reactor under 1000 atm pressure where the fuel temperature is 35,000° K and the hydrogen propellant temperature is 17,500° K at a mass flow rate of 4.5 kg/s, we find that λ_C = 75 cm and the e-folding time is 0.9 seconds. Because the critical wavelength, λ_C, is smaller than the radius of the core, it is clear that such a system will support this instability, which could lead to serious loss of the fuel in relatively short times if not corrected. It should be noted also that the results given by Eqs. (8) and (10) are conservative, since they do not take into account the ionization that results from the fission energy. As will be noted later, these effects can be sizable, and make the growth rate significantly higher.

The mean velocity of the hydrogen in the above example which is commensurate with a mass flow rate of 4.5 kg/s is approximately 5 m/s. If once again we assume that the uranium in the core is stationary, then the relative flow of the hydrogen to the fuel gives rise to the hydrodynamic instability known as the Kelvin-Helmholtz instability[8], whose onset condition is given by

$$v_h^2 > \frac{g}{k_V}\frac{(\rho_U^2 - \rho_h^2)}{\rho_U\rho_h} \approx \frac{g\rho_U}{k_V\rho_h} \qquad (11)$$

where v_h is the propellant velocity, ρ_h its mass density, and k_V the wavelength of the oscillation. For the example cited above, it can be shown[6] that such an instability can lead to loss of the uranium fuel at a rate of approximately 3% per second, which is clearly large and unacceptable.

Both of these instabilities lend themselves to stabilization by magnetic fields. It can be shown[9] that if a magnetic field B is introduced in the direction of the propellant flow, then it can act as a "surface tension" type of force that provides stability if the following condition is satisfied:

$$\frac{\rho_U\rho_h}{(\rho_U + \rho_h)}v_h^2 \le \frac{B^2}{8\pi} \qquad (12)$$

If applied to the example discussed earlier, the above condition reveals that a minimum magnetic field strength of 54 Gauss is required. The shape of such a field that lends itself to confinement of the uranium plasma appears to be at first glance "mirror-like"[10] since such geometry might provide containment of the fuel and yet allow the propellant to exit through the nozzle. The field in this configuration is stronger at the ends than it is at the center where the uranium core is to be situated. The ratio of the field strength at the "mirror" where the plasma particles are reflected to that at the center is referred to as the mirror ratio R_M. The higher the value of such a parameter, the smaller is the loss of particles through the mirrors. For GCR, a slight degree of asymmetry in the value of R_M would be required to inhibit the loss of uranium from the end that is opposite to the nozzle. Complete confinement of the fuel by this scheme is impossible since that requires an infinite mirror ratio, but significant reduction in the losses can be achieved with moderate values of R_M. To fully address mirror containment of GCR fuel requires solving a set of time-dependent conservation equations[11] for all the species involved, namely uranium ions, fission fragment ions, and the electrons. These equations take into account, among other things, the buildup of electron density as a

result of continuous ionization of the uranium and fission fragment ions, as well as the energy exchange between all these particles. These calculations are too lengthy for the purposes of this paper; the effectiveness of this magnetic confinement scheme can however be crudely assessed by directly applying the confinement law often used for fusion plasma[12] to GCR, namely

$$\frac{N_U}{\tau_U} = \frac{(3.84388\times10^{-12})N_U^2 Z_U^2}{E_U^{3/2}\log_{10}(R_M/[1+Z_U e\Phi/E_U])} \qquad (13)$$

where τ_U is the confinement time, eZ_U the effective charge of the uranium ions whose mean energy is denoted by E_U, and Φ is the electrostatic potential that builds up in the device as a result of the rapid loss of the electrons through the mirrors. By substituting appropriate numbers in the above equation, we get an idea as to whether magnetic mirrors can provide the added containment of the fuel in the GCR reactor noted earlier. Table 1 shows some of the results for a mirror ratio R_M of 100.

Table 1
Magnetic Mirror Containment of Uranium Ions

E_U (keV)	Z_U	N_U (cm^{-3})	$e\Phi$ (keV)	N_U/τ_U (cm^{-3}-sec^{-1})
0.002	1.8	1.53×10^{17}	0.0076	9.823×10^{27}
0.010	5.8	1.53×10^{17}	0.0206	1.175×10^{28}
0.050	18.0	1.53×10^{17}	0.0438	1.089×10^{30}
100.000	92.0	1.53×10^{17}	9.1476	6.274×10^{27}
500.000	92.0	1.53×10^{17}	43.1815	5.492×10^{26}

We note from the last column that such a magnetic configuration is ineffective in confining the fuel, perhaps because Eq. (13) may not be appropriate. In fact, this confinement law is only applicable to a fusion-type plasma such as DT where the density and charge are quite low compared to those in GCR. Under GCR conditions, it can readily be shown[11] that the particle-particle collision time is much shorter than the transit time, and as a result magnetic mirror confinement as represented by Eq. (13) is inapplicable. The use of this or other magnetic configurations must be examined in detail to ascertain their suitability for GCR containment.

It is often noted[7] that the 7.5 GW reactor alluded to earlier will produce an I_{sp} of 5000 s at a propellant flow rate of about 5 kg/s. But that does not take into account the heat flux limitation and the temperature of the solid wall that surrounds the core cavity. To assess these effects, we employ a heat transfer model[13] which assumes that the fuel core is cylindrical in shape with a radius of 1 m, axial length of 2 m, and an outer wall radius of 1.2 m. A modified version of Eqs. (2) - (4) that are applicable to the hydrogen propellant are

$$\frac{\partial\rho_h}{\partial t} + \vec{\nabla}\cdot\rho_h\vec{v}_h = 0 \qquad (14)$$

$$\rho_h\frac{D\vec{v}_h}{Dt} = -\vec{\nabla}p - \vec{\nabla}\cdot\vec{\bar{S}} + \rho_h\vec{g} \qquad (15)$$

$$\rho_h C_{ph}\frac{DT_h}{Dt} = -(\vec{\nabla}\cdot\vec{q}) + \frac{Dp}{Dt} + \vec{\bar{S}}:\vec{\nabla}\vec{v}_h \qquad (16)$$

where ρ_h and $\vec{v}_h$ are respectively the mass density of the hydrogen and its mean velocity. $\vec{\bar{S}}$ is the stress tensor, q the heat flux, C_{ph} the specific heat, and $\vec{g}$ represents the acceleration associated with external forces. If we limit our analysis to a steady state, inviscid flow with constant pressure and no external forces, then the momentum Eq. (15) is automatically satisfied. Furthermore, if we assume that the fluid properties remain nearly constant, and invoke azimuthal symmetry, then the energy Eq. (16) reduces to, in cylindrical coordinates:

$$\rho_h C_{ph}\left(v_{zh}\frac{\partial T_h}{\partial z} + v_{rh}\frac{\partial T_h}{\partial r}\right) = -\frac{1}{r}\frac{\partial}{\partial r}(rq_r) + P_f \qquad (17)$$

The radial velocity v_r can be ignored except in cases where transpiration cooling is required. Once again we will adopt the diffusion method of heat transfer, so that we can write

$$q_r = -k\frac{\partial T}{\partial r} \qquad (18)$$

where we have removed the subscript h since it is no longer needed for the current discussion pertaining to the propellant. The heat transfer coefficient k in the above equation is composed of a conduction part and a radiation part: i.e.

$$k = k_{cond} + k_{rad} = k_{cond} + K_R \qquad (19)$$

where the last term is the same as Eq. (16). We apply this analysis to the reactor mentioned earlier, along with the input parameters shown in Table 2.

Table 2
GCR Heat Transfer Input Parameters

Reactor Power	7.5 GW
Reactor Pressure	1000 atm
Max. Wall Heat Flux	100 MW/m^2
Inlet Prop. Flow Rate	5.0 kg/s
Inlet Temperature	2200° K
Wall Temperature	2200° K
Fuel/Prop. Flow Ratio	10/1

The results are given in Table 3

Table 3
Results of Heat Transfer Model

Fuel Reservoir Temperature	76,790° K
Prop. Reservoir Temperature	18,450° K
Wall Cooling Flow	1.3 kg/s
Specific Impulse	3362 s
Thrust	207 kN

The variation of I_{sp} with mass flow rate for different maximum wall heat fluxes is shown in Fig. (3). We see that if there is no limit on q_{wall}, then I_{sp} increases as the flow rate decreases until a maximum of 4800 s is reached. This maximum indicates that the propellant has reached an equilibrium temperature, meaning that any additional energy generated in the fuel will be conducted to the wall. If a maximum wall heat flux is specified, then I_{sp} reaches a peak at some optimum flow rate. If the inlet flow is reduced below this value, then transpiration cooling would be

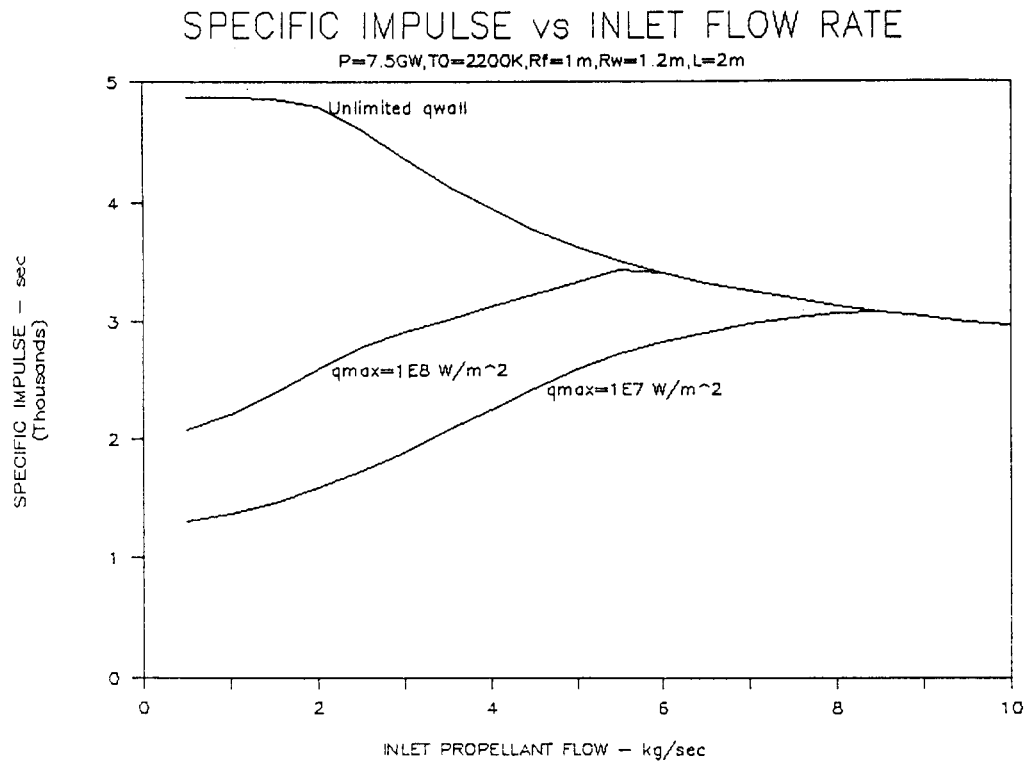

Fig. 3

required, thus lowering the specific impulse.

Another critical issue that could seriously detract from the propulsive merits of GCR is the turbulent mixing of fuel and propellant. A preliminary study of this phenomenon[14] shows that a 500 MW reactor with a 10/1 propellant-fuel (P/F) mass flow ratio produces almost the same I_{sp} as a 1000 MW reactor with a 2/1 P/F ratio, with a comparable propellant mass flow rate of about 4 kg/s. Although the thrust in the second case was about twice that of the first, the fact remains that a higher mixing ratio results in such a substantial axial drop in the fuel volume fraction or the fuel mass fraction that criticality was not achievable.

Physics Basis of MICF

The dynamics of the plasma in MICF is governed by a coupled set of quasi-one dimensional, time dependent conservation equations that include radiation transport from the hot plasma to the various regions of the pellet, as well as particle and energy transport across the magnetic field between the hot core and the cold plasma region (halo) in both directions as illustrated in Fig. (2). These equations are too lengthy to be included in this paper, but to illustrate the various phenomena involved, we present the particle and energy conservation equations for the fuel ions, i.e. deuterium and tritium, which we will treat as one species with an average mass of 2.5 atomic mass units. These equations are[4]:

$$\frac{d}{dt}\left\{\frac{4}{3}\pi r^3 n_f\right\} = -\frac{4}{3}\pi r^3\left\{\frac{1}{2}n_f^2<\sigma v>\right\} + 4\pi r^2(\Gamma_r-\Gamma_f) \quad (20)$$

$$\frac{d}{dt}\left\{\frac{\frac{4}{3}\pi r^3 n_f T_f}{\gamma-1}\right\} + 4\pi r^2 n_f T_f\frac{dr}{dt} = \frac{4}{3}\pi r^3\left\{\frac{3}{2}\frac{n_f n_e}{(n\tau)_{ef}}(T_e-T_f) + \frac{3}{2}\frac{n_f n_\alpha}{(n\tau)_{\alpha f}}(T_\alpha-T_f) + n_f n_{f\alpha}\left(\frac{dE_{f\alpha}}{dt}\right)_f - \frac{3}{4}n_f^2 T_f<\sigma v>_f\right\} + 4\pi r^2(W_r-W_f) \quad (21)$$

In these equations, n_f and T_f denote respectively the fuel ion density and temperature, $<\sigma v>_f$ the velocity-averaged fusion reaction cross section which is temperature dependent, Γ_r the particle flux for the refueling ions which cross the magnetic field from the halo region to the core plasma, and Γ_f the flux in the opposite direction. The left hand side of Eq. (21) represents the change in the thermal energy of the plasma, including the spherical expansion, treating it as an ideal gas with the

adiabatic constant $\gamma = 5/3$. The terms that contain temperature differences denote the energy exchange between the fuel ions and the other species, e.g. electrons and thermal alpha particles, where such an exchange is characterized by the exchange parameter $(n\tau)$. $(dE_{f\alpha}/dt)_f$ is the rate at which energy given to a typical fuel ion by a single fusion alpha particle as it slows down from its initial 3.5 MeV energy. The term containing $<\sigma v>_f$ denotes the removal of two ions, with their attendant energy, from the fuel ion population for each fusion event. The energy transport terms across the magnetic field are identified by W_e and W_f in exactly the same way as Γ_e and Γ_f have been defined. Solution of the underlying equations yields, among other things, the energy enhancement factor, Q, which denotes the energy produced by the fusion reactions per unit of input energy. An illustrative set of results is given in Table 4.

Table 4

MICF Pellet Design for Propulsion

Inner Radius of Solid Fuel	0.25 cm
Outer Radius of Solid Fuel	0.30 cm
Outer Radius of Metal Shell	0.547 cm
Fusion Fuel	DT
Hot Plasma Core Density	5×10^{21} cm^{-3}
Initial Plasma Core Temperature	10 keV
Input Laser Energy	2.59 MJ
Gain Factor	724
Pellet Mass	8.75 g

A propulsion system based on MICF is illustrated in Fig. (4), where the target pellet is ignited by a laser beam (or other drivers) in a reaction chamber, and the hot plasma is exhausted at the end of the burn through a magnetic nozzle to generate the thrust. An especially convenient nozzle in this regard is the "meridional" nozzle[15] which is cylindrically symmetric and does not allow for an azimuthal component in either the magnetic field or the fluid velocity. It assumes that the fluid (plasma) moves along the magnetic field lines which constrict at the throat and open up at the exit so that the flow can be governed by the Bernoulli Equation:

$$\frac{v_f^2}{2} + \frac{\gamma}{\gamma - 1}\frac{p_f}{\rho_f} = C \qquad (22)$$

where v_f, p_f, and ρ_f are respectively the fluid velocity, pressure, and density, γ the adiabatic constant introduced earlier, and C is a constant. For such a nozzle, the thrust F and the specific impulse I_{sp} can be written as

$$F = \frac{5}{3} A_0 p_R$$

$$I_{sp} = \frac{\sqrt{3} C_{sR}}{g} \qquad (23)$$

where A_0 is the area of the nozzle throat, C_{sR} the sound speed at the reservoir (where the fusion energy is produced), and g the gravitational acceleration. Applying these results to the MICF pellet presented earlier, we find that the corresponding propulsion system has the characteristics given in Table 5.

Table 5

MICF Propulsion System

DT Ion Exhaust Velocity	375 km/s
Metal (Tungsten) Ion Exhaust Velocity	43.8 km/s
Effective I_{sp}	0.451×10^4 s
Repetition Rate ω	$\leq$ 6422 Hertz
Total Thrust F	0.172ω kN
Jet Power	4.046ω MW

In obtaining the above results, we assumed that the plasma, including the metal shell ions, expands adiabatically in a reaction chamber of 100 cm radius, and escape through a nozzle of throat radius 2.5 cm. For a rep rate of 10, this propulsion system produces about 2 kN of thrust and 40 MW of jet power with a specific impulse of about 4500 s. It is interesting to note that a wide range of propulsive properties can be obtained in MICF by simply varying the design of the pellet. A longer or shorter burn time can be achieved by changing the thickness of the metal shell in the target, since that dictates the lifetime of the burning plasma. Moreover, the choice of the metal shell material itself also dictates the relative values of specific impulse and thrust that can be generated.

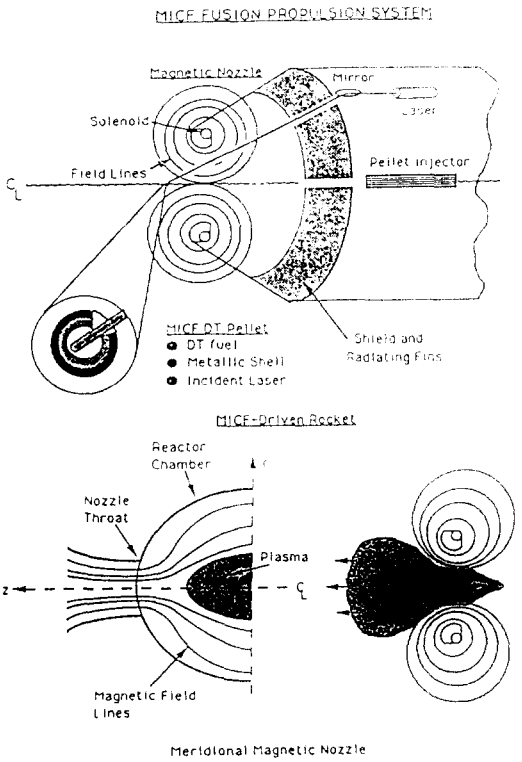

Fig. 4
Schematic of MICF Rocket and Magnetic Nozzle

Although the above MICF results were obtained for an input laser energy of about 2.5 MJ, it has been shown[4] that similarly good propulsive results can be achieved with less input energy. However, there is a lower limit below which ignition and energy enhancement cannot be achieved. This, in turn, means that laser technology will have to progress to the point where it can be readily used in an MICF propulsion system. Because of the large power supply and other auxiliary systems that are required for a laser-driven fusion system of this magnitude, the corresponding dry weight for such a rocket will be quite large, and perhaps prohibitively costly. An alternative ignition system that can do away with these restrictions would certainly be most welcome. The use of anti-hydrogen annihilation for triggering fusion reactions in MICF would be especially attractive, since very small amounts will be needed to initiate reactions in targets such as those described above[16].

Conclusion

We have examined in this paper two nuclear propulsion systems that have the potential for rapid interplanetary travel. Both of these systems can, in principle, generate large enough specific impulses and thrusts to allow a manned mission to Mars, for example, to be completed in a few months instead of years. The open cycle gas core fission rocket has been advanced as a system that can produce I_{sp} ~ 5000 s and thrusts of about 200 kN. But we have seen that such propulsive capabilities would be hard to achieve if material heat load limitations are taken into account, and other hydrodynamic phenomena that lead to turbulent mixing and rapid depletion of fuel are not addressed. Although some of these phenomena lend themselves to correction by magnetic fields, it was shown that certain magnetic geometries do not provide the added desired containment, and further work is needed in this area. The MICF fusion system takes advantage of a self generated magnetic field that allows the plasma to burn for a relatively long time, and thus produce sizable energy magnification through the fusion reactions initiated inside the target. The system, i.e. the fuel ions and the metal shell ions, turns into a hot plasma at the end of the burn, and with the aid of a magnetic nozzle these particles get exhausted to generate the thrust. In contrast to GCR, the fusion system uses the same plasma particles as fuel and propellant, thereby circumventing some of the problems that arise when fuel and propellant are different. The MICF system also appears to be less complicated than GCR and can produce equally as good if not better propulsion parameters. A major concern for MICF, however, is the large laser energies needed to ignite the pellets; but preliminary studies have shown that they can be reduced significantly with careful target design. Clearly, a better solution would be to do away with these massive drivers and replace them with tiny "sparks" such as anti-hydrogen pellets that can initiate the fusion reactions; but these approaches must await further research and development.

Acknowledgement

This work was supported in part by the U. S. Department of Energy.

References

1. T. Kammash and D. L. Galbraith, AIAA-91-3650, AIAA/NASA/OAI Conference on Advanced SEI Technologies, Cleveland, OH Sept. 4 - 6 (1991)
2. R. G. Ragsdale, Nuclear Thermal Propulsion, A Joint NASA/DOE/DOD Workshop, Cleveland, OH July 10 - 12 (1990)
3. A Hasegawa et al, Nuclear Fusion 28, 369 (1988)
4. T. Kammash and D. L. Galbraith, Nuclear Fusion 29, 1079 (1989)
5. R. G. Ragsdale and E. A. Willis Jr, AIAA-71-641, *7th* Propulsion Joint Specialist Conference, Salt Lake City, UT June 14 - 18 (1971)
6. T. Kammash and D. L. Galbraith, AIAA-92-3818, *28th* Joint Propulsion Conference, Nashville, TN July 6 - 8 (1992)
7. S. K. Borowski, NASA Technical Memorandum 101354, July 18 (1987)
8. S. Chandrasekhar, Hydrodynamic and Hydromagnetic Stability, Dover Publications, N.Y. (1961)
9. T. Northrop, Physical Review 103, 1150 (1956)
10. T. Kammash, Fusion Reactor Physics Principles and Technology, Ann Arbor Science Publishers (1975) Ch. 2
11. T. Kammash and D. L. Galbraith, AIAA-93-2368, *29th* Joint Propulsion Conference, Monterey, CA, June 28 - 30 (1993)
12. R. F. Post, Nuclear Fusion 27, 1579 (1987)
13. D. I. Poston and T. Kammash, Proc. *9th* Symp. on Space Nuclear Power, American Institute of Physics CONF 920104, p 1083 (1992)
14. D. I. Poston, Private Communication
15. R. Gerwin et al, Astronautics Laboratory (AFSC) Report AL-TR-89-092, February (1990)
16. T. Kammash and D. L. Galbraith, J. Propulsion and Power 8, 644 (1992)